JOURNAL OF APPLIED POLYMER SCIENCE VOL. 8, PP. 3–24 (1964)

Effect of Rate and Temperature on the Tensile Properties of Double-Base Propellant

E. McABEE and M. CHMURA, *U. S. Army Munitions Command, Picatinny Arsenal, Dover, New Jersey*

Synopsis

The tensile properties of two cast and two extruded solid rocket propellants were studied at 25°C. and 50% R.H. over a range of failure times from 0.005 to 2500 sec. The effects of temperature were also investigated at the highest rate and at 0.1 in./in./min. over a range of −60 to 80°C. The results indicate that both temperature and rate of loading greatly affect the tensile properties of double-base propellants.

Because of the increased use of materials in applications where the maximum load is applied in short times, and the necessity from both practical design and economic consideration to maintain a high pay load to weight ratio, greater emphasis is being placed on the mechanical properties of these materials as observed under short time loading. All viscoelastic materials are known to exhibit a marked degree of both time and temperature sensitivity. Solid rocket propellants are examples of such materials.

In order to study the effects of a wide range of failure times and temperatures, on the tensile behavior of solid propellants four representative formulations were selected. The test method and equipment used are described in Appendix I. Two cast materials (OGK and ARP) and two extruded materials (T-16 and X-8), considered to be representative of the extremes of rigidity of cast and extruded double-base propellants, were selected for examination. The type specimen used is described in Appendix II.

The first portion of the investigation was directed toward determining the behavior of these materials at 25°C. and 50% R.H. over a range of failure times of from approximately 0.005 to 2500 sec. Accordingly, the gas flow and pressure (Appendix I) were adjusted to produce failure in times of approximately decade increments. Table I and Figures 1–4 show the effect of rates of loading on the four formulations studied.

The plots of tensile strength versus time to failure (Fig. 1) show curves of a similar shape but with different degrees of curvature. With the exception of T-16, all of these plots show a tendency to level off and quite possibly all might show a decrease in strength, as exhibited by OGK, if the rate of loading were sufficiently increased.

TABLE I
Effect of Rate of Loading on the Tensile Properties of Double-Base Propellant at 25°C.

			OGK					
Time to failure (sec.)	1600	172	17.9	1.73	0.79	0.093	0.012	0.005
Modulus at 1% (psi)	31,700	35,000	43,800	52,000	65,000	71,000	93,000	106,000
Tensile strength (psi)	963	1270	1720	2260	2540	3050	3820	3720
Maximum elongation (%)	27.4	28.6	29.8	28.2	25.0	14.7	6.9	5.3
Work to produce failure (ft.-lb./in.^{3})	18.3	25.1	35.0	46.1	46.8	30.1	14.7	9.6
			ARP					
Time to failure (sec.)	2590	338	34.8	1.50	0.68	0.13	0.013	0.007
Modulus at 1% (psi)	3900	4650	8030	9500	17,000	27,000	30,000	35,600
Tensile strength (psi)	265	441	864	1620	1940	2550	3150	3190
Maximum elongation (%)	43.1	56.4	58.0	65.0	61.3	50.2	38.5	35.1
Work to produce failure (ft.-lb./in.^{3})	7.6	15.5	27.5	56.8	64.1	71.9	64.3	46.4
			T-16					
Time to failure (sec.)	1104	132	13.0	1.59	0.58	0.10	0.014	0.006
Modulus at 1% (psi)	13,000	16,600	23,200	36,500	59,000	50,000	60,000	112,000
Tensile strength (psi)	507	702	1150	1805	2220	3030	3970	4470
Maximum elongation (%)	18.4	22.0	21.6	22.4	21.1	19.5	13.1	11.9
Work to produce failure (ft.-lb./in.^{3})	6.1	9.9	15.5	24.8	30.8	37.6	29.0	32.7
			X-8					
Time to failure (sec.)	606	83.4	12.4	1.55	0.40	0.08	0.015	0.005
Modulus at 1% (psi)	923	11,200	14,900	22,000	23,000	45,000	49,000	75,000
Tensile strength (psi)	305	447	694	1110	1660	2185	2990	3250
Maximum elongation (%)	10.1	13.9	20.7	29.4	18.0	20.5	20.6	19.6
Work to produce failure (ft.-lb./in.^{3})	1.0	3.8	9.0	21.4	17.4	26.5	33.3	38.4

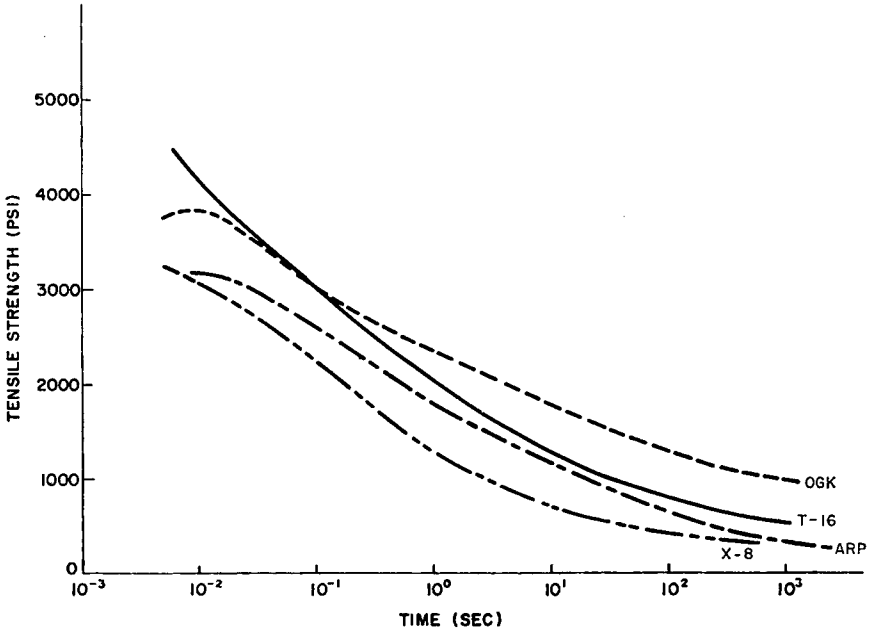

Fig. 1. Effect of rate of loading on the tensile strength of double-base propellant at 25°C.

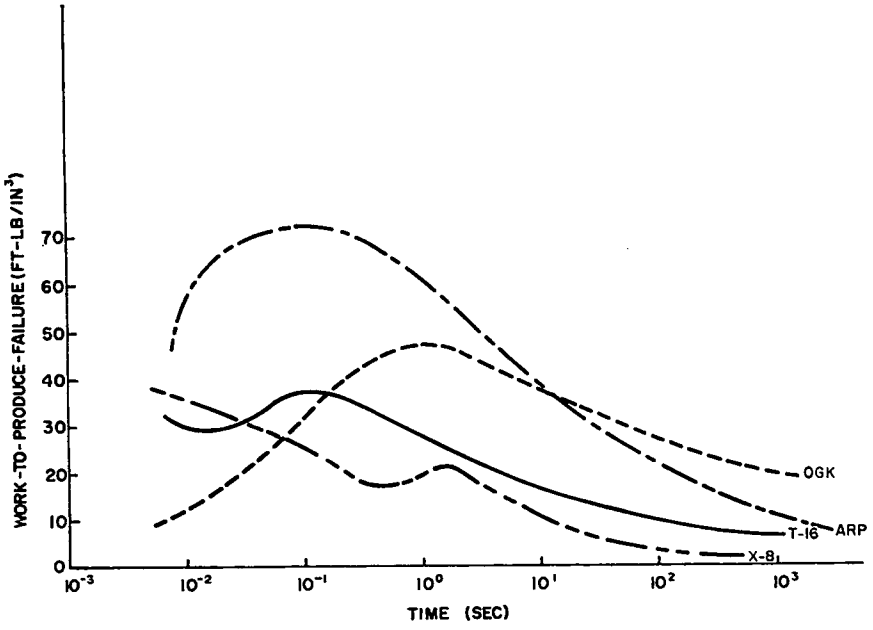

Fig. 2. Effect of rate of loading on the work-to-produce-failure of double-base propellant at 25°C.

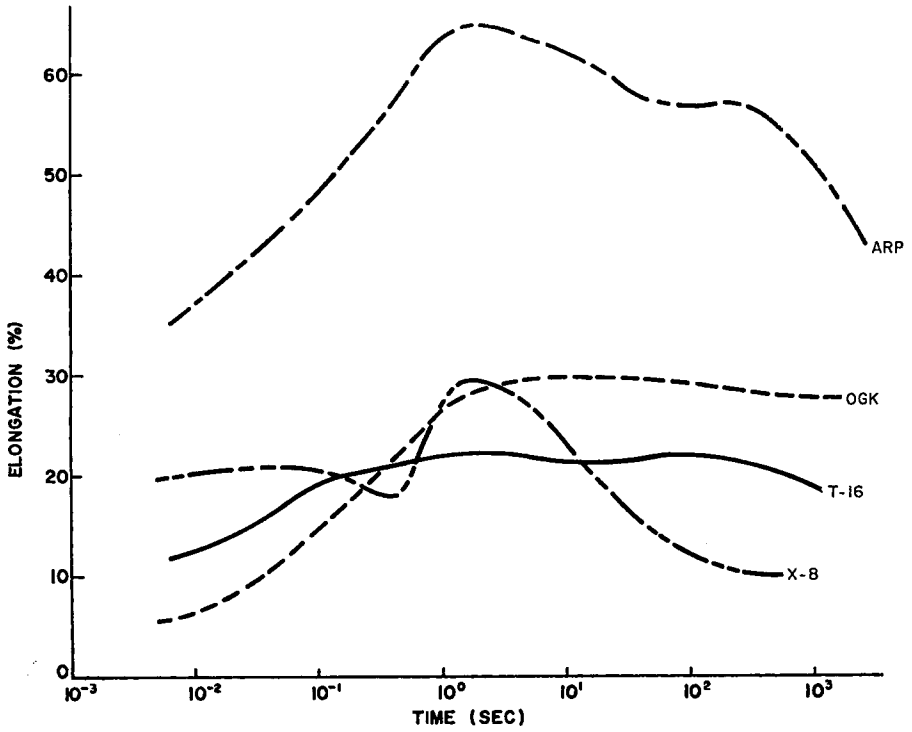

Fig. 3. Effect of rate of loading on the ultimate elongation of double-base propellant at 25°C.

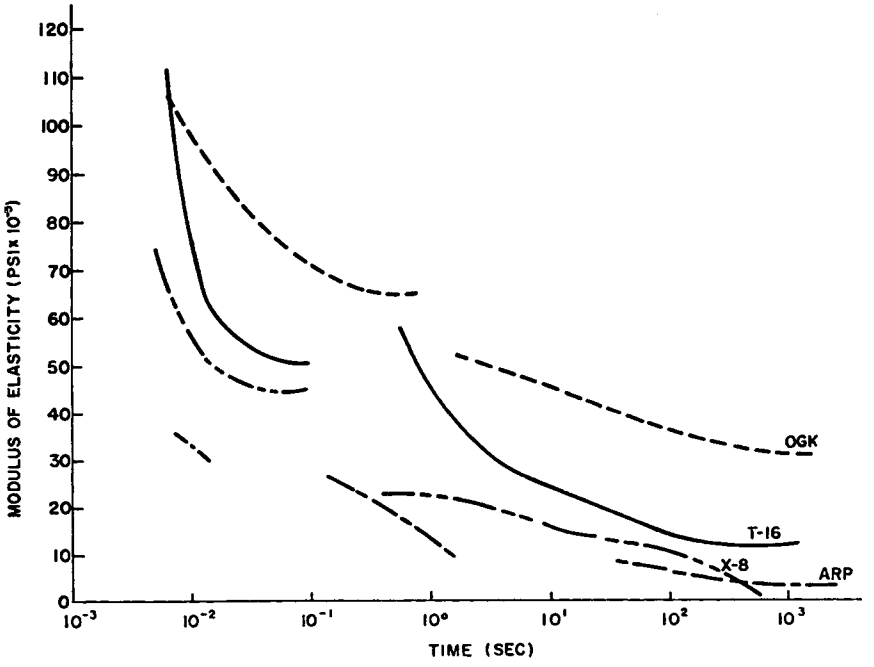

Fig. 4. Effect of rate of loading on the modulus of elasticity of double-base propellant at 25°C.

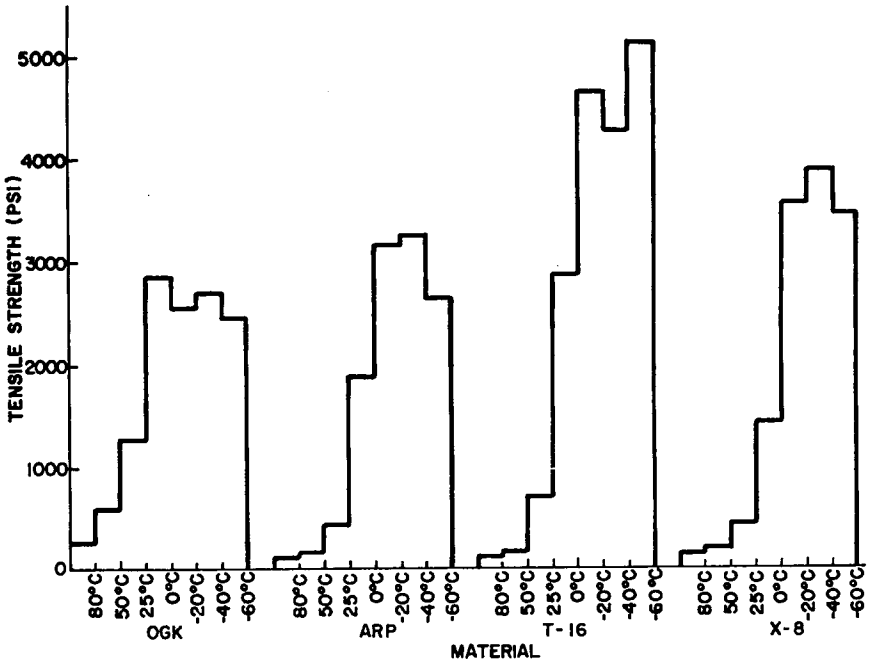

Fig. 5. Effect of temperature on the tensile strength of double-base propellant at static rates of loading (0.1 in./in./min.).

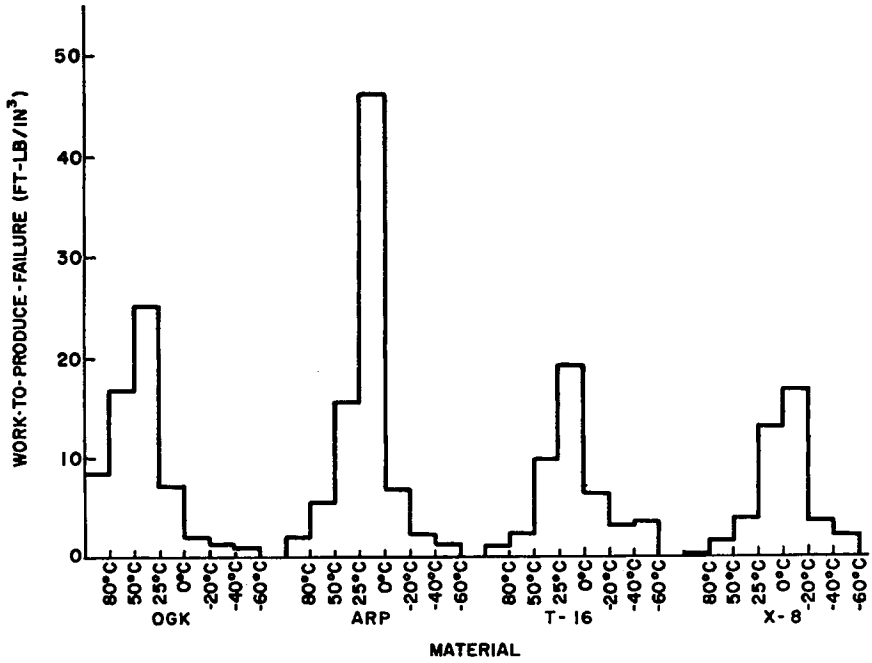

Fig. 6. Effect of temperature on work-to-produce-failure of double-base propellant at static rates of loading (0.1 in./in./min.).

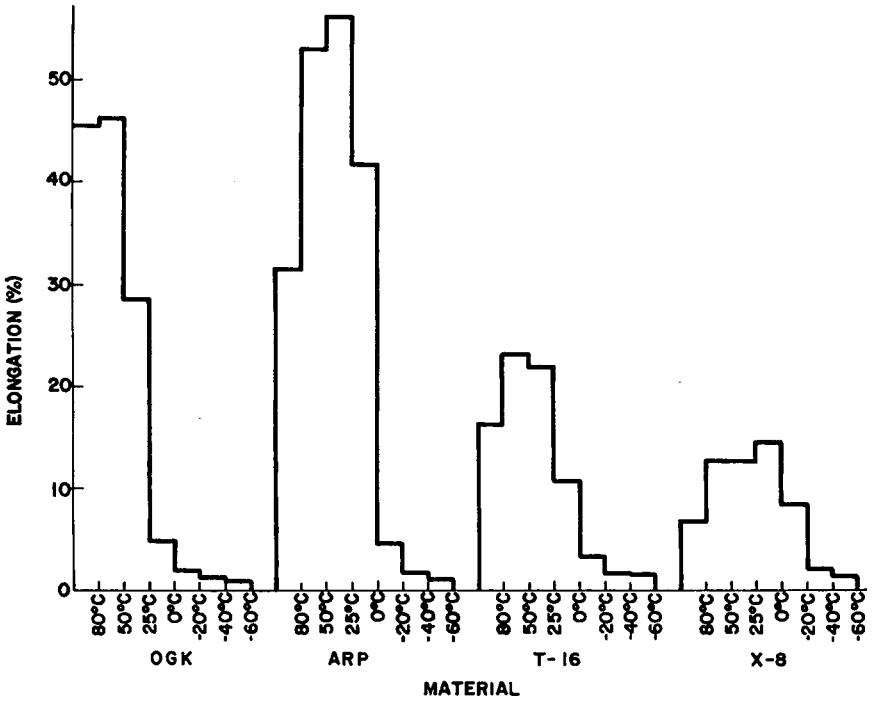

Fig. 7. Effect of temperature on ultimate elongation of double-base propellant at static rates of loading (0.1 in./in./min.).

The plot of work to produce failure versus log time (Fig. 2) shows some similarity between the two cast formulations (OGK and ARP) in that a maximum is reached at an intermediate rate. The maximums for both materials are not reached at the same rate. The two extruded formulations also show similar tendencies, but not at the same rate. Both reach a maximum, pass through a minimum, and then continue to increase with increasing rate. However, it cannot be stated whether or not the cast and extruded materials could be characterized by curves more nearly alike if the failure times were decreased sufficiently to allow a minimum to be reached for all.

The ultimate elongation curves (Fig. 3) show no general trend and are completely unpredictable.

The modulus of elasticity versus log time plot (Fig. 4) shows sharp breaks in all cases although these do not occur at the same rate. ARP shows a second discontinuity at a lower rate. The effect of rate on modulus is extremely unpredictable and clearly illustrates the risk of prediction of a value for use in design from data obtained at another rate.

The second portion of the investigation was directed toward studying the effect of temperature over a range from −60 to 80°C. The results obtained for the commonly reported properties at the conventional static rate (nominally 0.1 in./in./min.) are shown in Figures 5–8 and Table II.

TABLE II

Effect of Temperature on the Tensile Properties of Double-Base Propellant at 0.1 in./in./min.

			OGK				
Temperature (°C.)	80	50	25	0	−20	−40	−60
Time to failure (sec.)	275	278	172	30.1	11.8	7.9	6.4
Modulus at 1% (psi)	5120	11,100	35,000	75,600	130,000	211,000	235,000
Tensile strength (psi)	268	591	1270	2860	2540	2700	2450
Maximum elongation (%)	45.8	46.3	28.6	5.0	2.0	1.3	1.1
Work to produce failure (ft.-lb./in.^{3})	8.4	16.8	25.1	7.1	2.0	1.4	1.1
			ARP				
Temperature (°C.)	80	50	25	0	−20	−40	−60
Time to failure (sec.)	190	319	338	251	29.3	11.0	6.7
Modulus at 1% (psi)	911	1480	4650	28,000	83,400	177,000	235,000
Tensile strength (psi)	109	159	441	1890	3170	3250	2640
Maximum elongation (%)	31.6	53.2	56.4	41.9	4.9	1.8	1.1
Work to produce failure (ft.-lb./in.^{3})	2.0	5.5	15.5	46.1	6.8	2.2	1.2
			T-16				
Temperature (°C.)	80	50	25	0	−20	−40	−60
Time to failure (sec.)	98	140	132	64.2	20.3	10.4	10.0
Modulus at 1% (psi)	1410	2480	16,600	71,700	137,000	245,000	308,000
Tensile strength (psi)	126	170	702	2870	4640	4260	5120
Maximum elongation (%)	16.4	23.3	22.0	10.7	3.4	1.7	1.7
Work to produce failure (ft.-lb./in.^{3})	1.1	2.3	9.9	19.1	6.3	3.1	3.4
			X-8				
Temperature (°C.)	80	50	25	0	−20	−40	−60
Time to failure (sec.)	41.0	76.8	83.4	88.2	51	13.4	8.5
Modulus at 1% (psi)	3840	4210	11,200	34,000	80,500	173,000	243,000
Tensile strength (psi)	150	207	447	1440	3550	3870	3450
Maximum elongation (%)	6.8	12.8	13.9	14.7	8.5	2.2	1.4
Work to produce failure (ft.-lb./in.^{3})	0.56	1.5	3.8	12.8	16.6	3.5	2.1

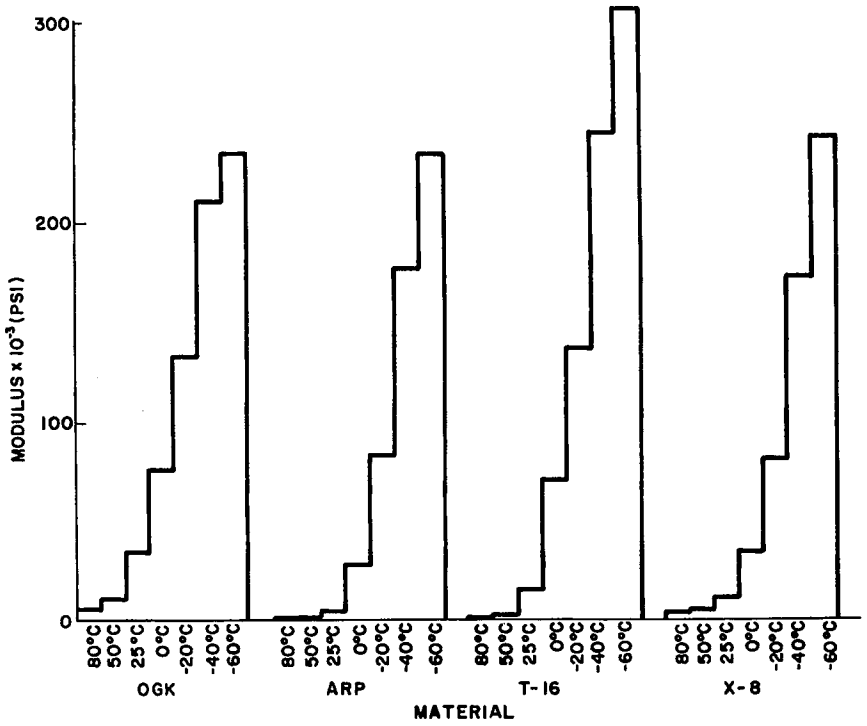

Fig. 8. Effect of temperature on modulus of elasticity of double-base propellant at static rates of loading (0.1 in./in./min.).

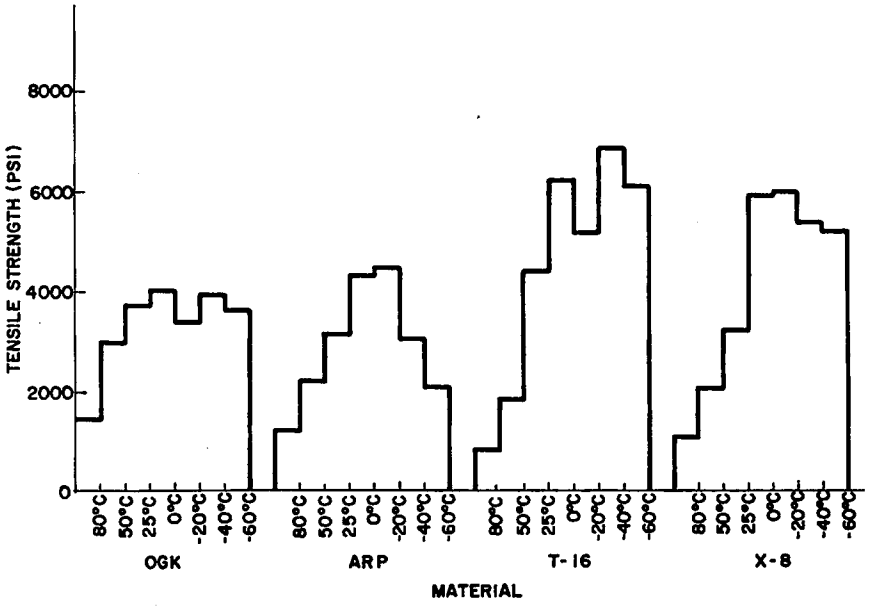

Fig. 9. Effect of temperature on tensile strength of double-base propellant at high rates of loading.

TABLE III

Effect of Temperature on the Tensile Properties of Double-Base Propellant at High Rates

			OGK				
Temperature (°C.)	80	50	25	0	−20	−40	−60
Time to failure (milliseconds)	6.5	5.0	5.0	2.0	3.5	1.3	1.0
Modulus at 1% (psi)	13,000	60,000	106,000	175,000	203,000	196,000	174,000
Tensile strength (psi)	1440	3000	3720	4130	3400	3980	3650
Maximum elongation (%)	45.4	29.3	5.3	2.4	3.6	2.0	2.1
Work to produce failure (ft.-lb./in.^{3})	37.4	55.0	9.6	4.1	7.4	3.3	3.2
			ARP				
Temperature (°C.)	80	50	25	0	−20	−40	−60
Time to failure (milliseconds)	7.5	7.0	7.7	3.0	2.5	1.0	1.0
Modulus at 1% (psi)	8000	13,000	35,600	43,000	180,000	130,000	150,000
Tensile strength (psi)	1240	2250	3190	4350	4500	3090	2150
Maximum elongation (%)	66.2	52.5	35.1	13.0	3.8	2.4	1.4
Work to produce failure (ft.-lb./in.^{3})	44.6	61.8	46.4	26.7	8.5	2.6	1.3
			T-16				
Temperature (°C.)	80	50	25	0	−20	−40	−60
Time to failure (milliseconds)	4.5	4.5	6.3	4.5	3.5	2.3	1.8
Modulus at 1% (psi)	3000	13,000	112,000	220,000	380,000	365,000	370,000
Tensile strength (psi)	857	1900	4470	6250	5200	6900	6130
Maximum elongation (%)	30.6	16.8	11.9	4.6	3.1	1.9	1.9
Work to produce failure (ft.-lb./in.^{3})	13.4	15.6	32.7	15.5	10.3	5.6	5.4
			X-8				
Temperature (°C.)	80	50	25	0	−20	−40	−60
Time to failure (milliseconds)	4.0	4.0	5.0	5.0	4.0	1.5	1.2
Modulus at 1% (psi)	8000	30,000	75,000	100,000	200,000	230,000	375,000
Tensile strength (psi)	1100	2100	3250	5950	6000	5400	5200
Maximum elongation (%)	28.1	21.0	19.6	8.5	3.0	2.4	1.4
Work to produce failure (ft.-lb./in.^{3})	17.5	26.0	38.4	26.1	7.3	5.3	3.1

This same effect of temperature at high rates is shown in Figures 9–12 and Table III. A comparison of the maximum and minimum values indicates that only the minimum strength and modulus occur at the same temperature for both rates.

The effect of loading rate on the overall shape of the stress-strain curve is shown in Figures 13 through 16. All of the materials except X-8 show a yield at the lower rates. This is followed by an increase in stress with OGK and T-16, while the ARP curves show a continued decrease in stress until failures occur. At the highest rate ARP shows this same tendency although no actual decrease in stress before failure is noted.

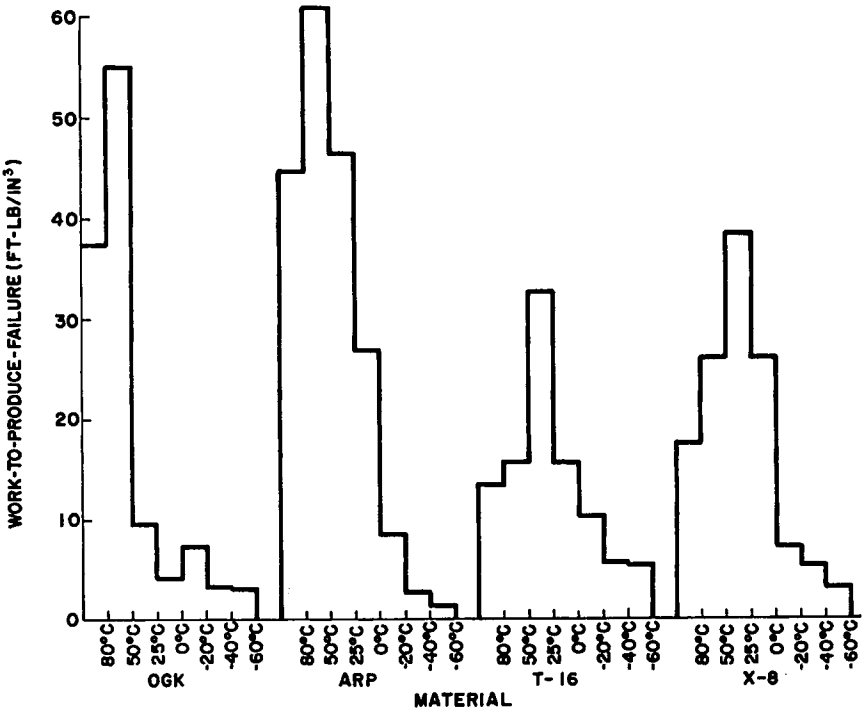

Fig. 10. Effect of temperature on work-to-product-failure of double-base propellant at high rates of loading.

Figures 17 through 20 show the effect of temperature on the stress-strain curves at the conventional testing rate of 0.1 in./in./min. In all cases, the higher temperature curves for each formulation are fairly similar and represent a not-too-marked change in values for the amount of temperature change. The lower temperature curves also show a certain degree of similarity and, for a similar change in temperature, less property variation. However, at some intermediate temperature, a decided change in the shape of the curve, as well as an increase in the distance between adjacent curves, may be noted.

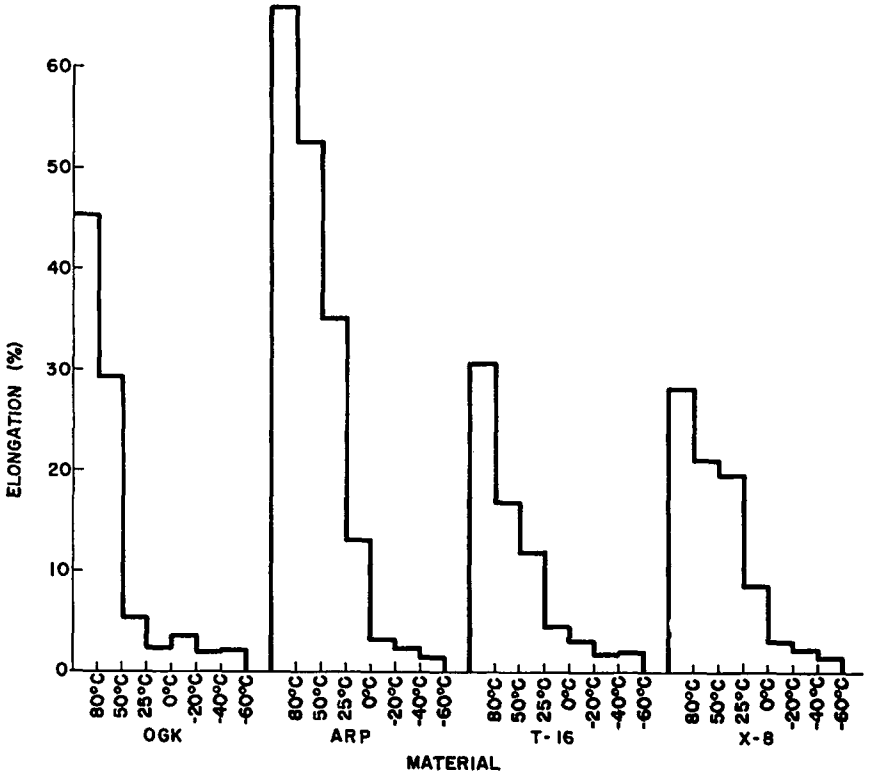

Fig. 11. Effect of temperature on ultimate elongation of double-base propellant at high rates of loading.

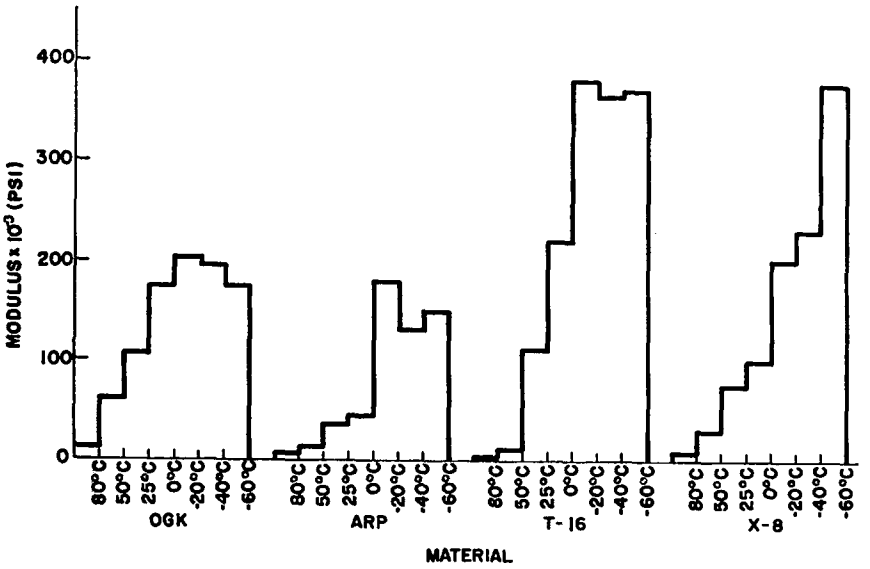

Fig. 12. Effect of temperature on modulus of elasticity of double-base propellant at high rates of loading

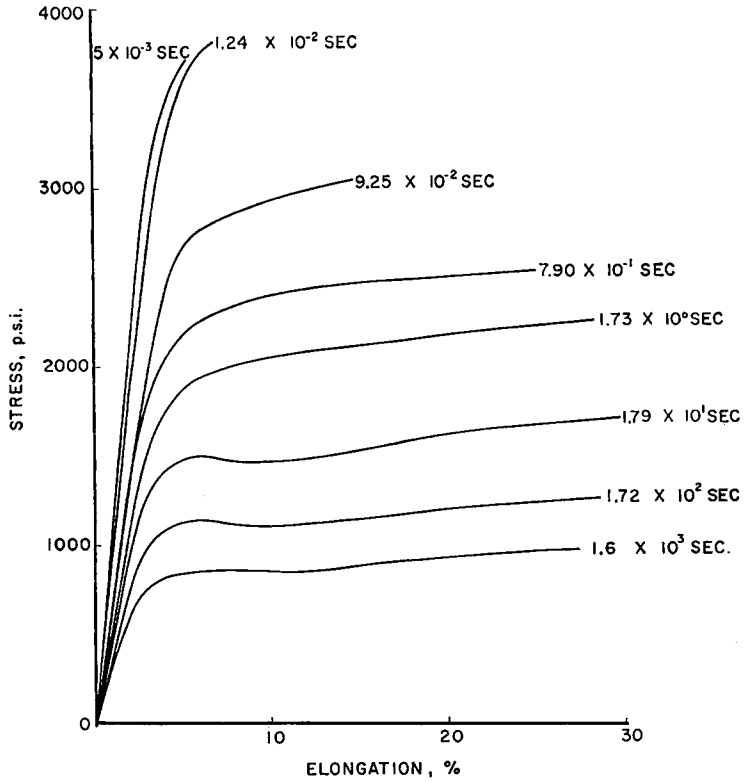

Fig. 13. Effect of rate on the stress-strain behavior of OGK at 25°C.

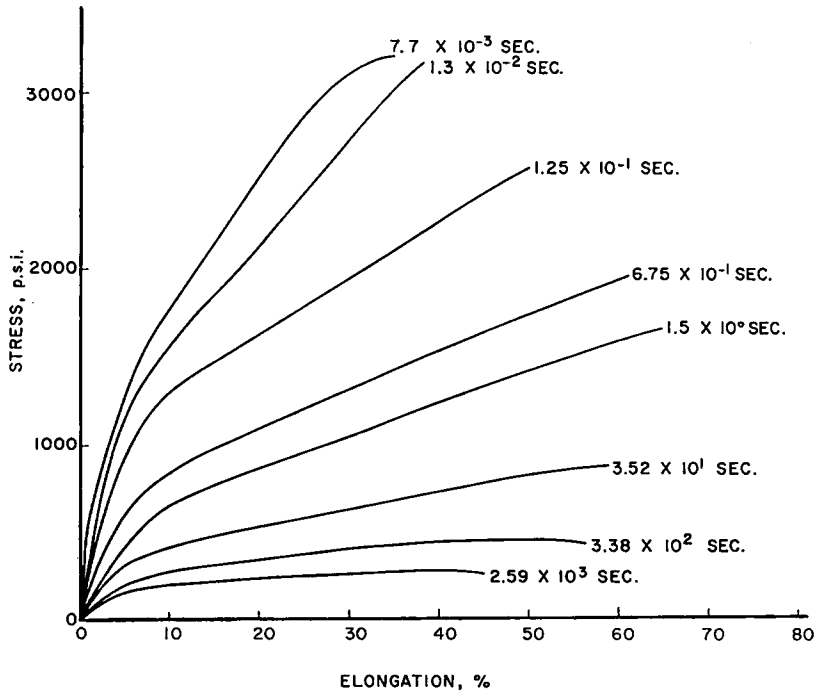

Fig. 14. Effect of rate on the stress-strain behavior of ARP at 25°C.

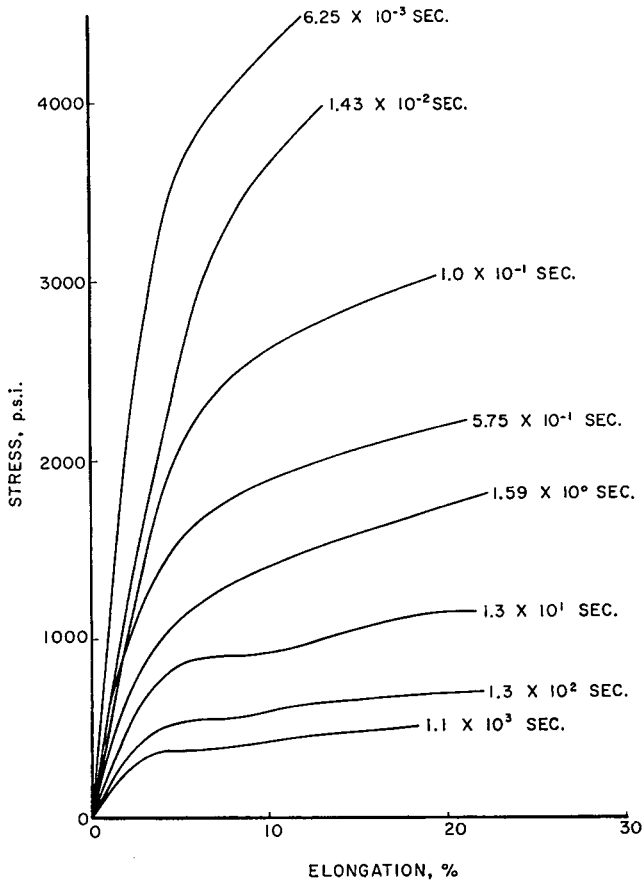

Fig. 15. Effect of rate on the stress-strain behavior of T-16 at 25°C.

Figures 21 through 24 show the effect of temperature on the stress-strain curves at the high rate of loading. The same tendency is shown as with the "static" tests. That is, at the higher temperature a similarity of shape is shown for any one material although the spread between curves is greater than at the "static" rates for corresponding temperatures. Again, at the lower temperatures, relatively little difference is noted between curves. This does not occur, however, at the same location as in the "static" tests.

The lack of any discernible trend in the results is probably due to interaction of several factors. For example, it is generally expected that as the rate of testing is increased and/or the temperature lowered, maximum strength will increase, modulus will increase, and elongation will decrease. This expectation is based on the belief that the individual molecules and molecular segments have less freedom of movement and so cannot readily rearrange themselves. However, as the rate of testing is increased, there is less opportunity for the heat built up to be dissipated

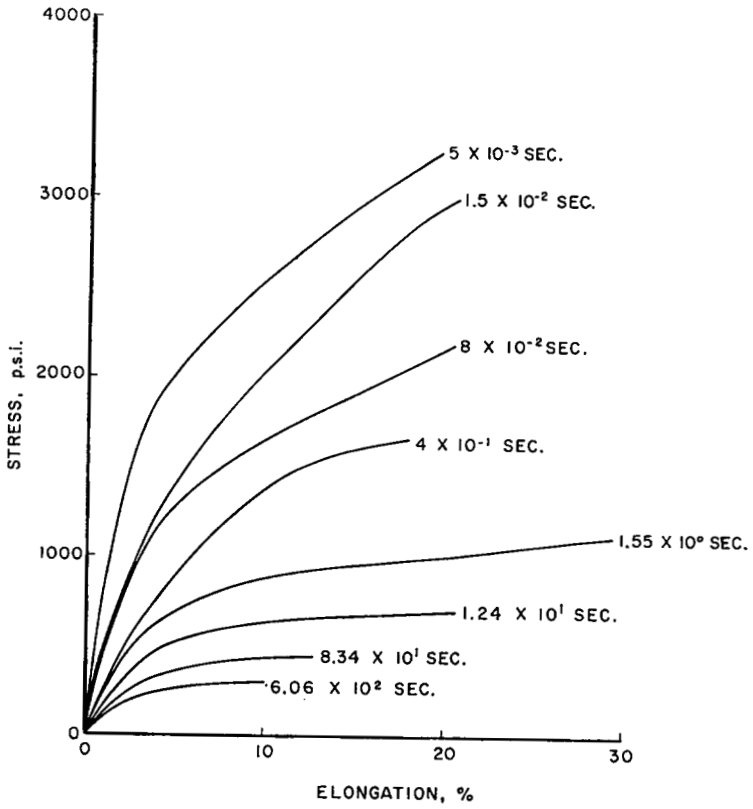

Fig. 16. Effect of rate on the stress-strain behavior of X-8 at 25°C.

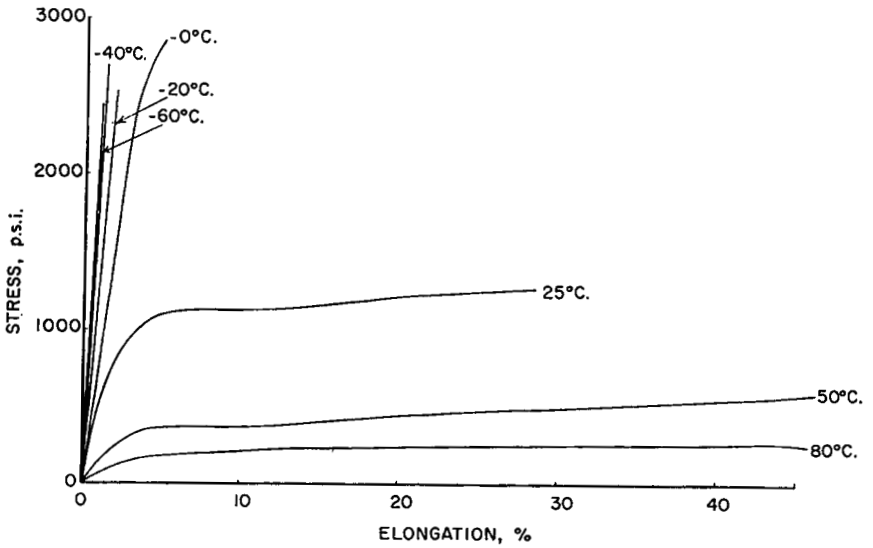

Fig. 17. Effect of temperature on the stress-strain behavior of OGK at 0.1 in./in./min.

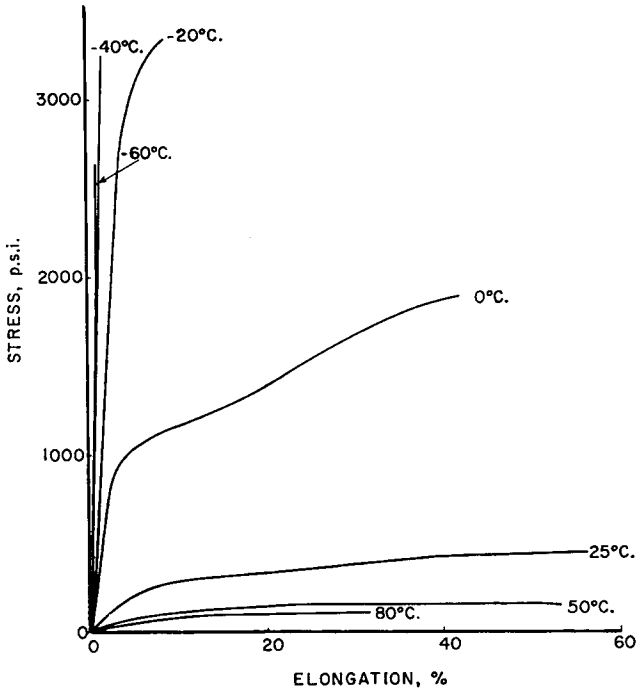

Fig. 18. Effect of temperature on the stress-strain behavior of ARP at 0.1 in./in./min.

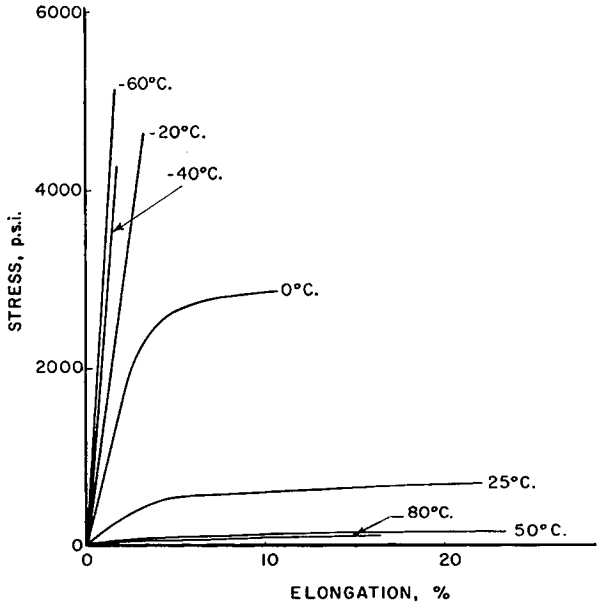

Fig. 19. Effect of temperature on the stress-strain behavior of T-16 at 0.1 in./in./min.

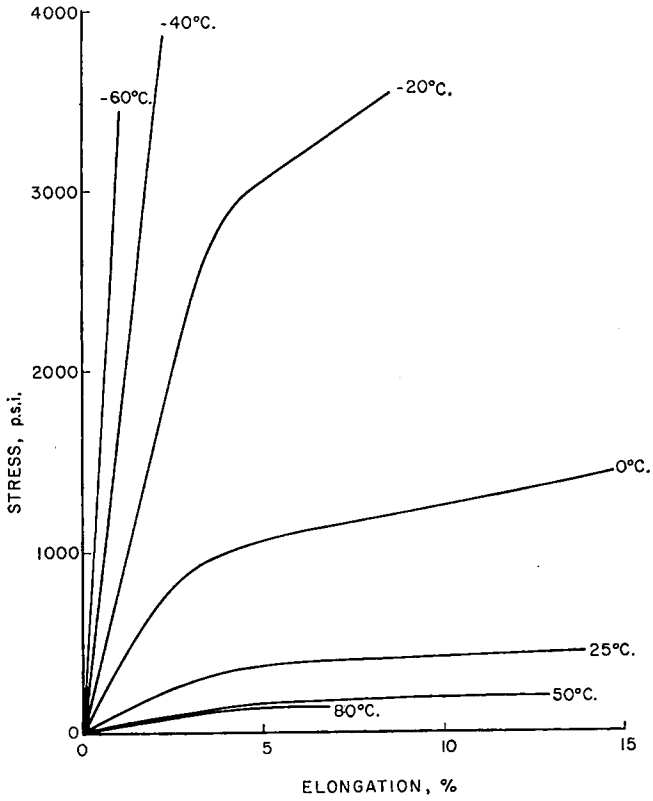

Fig. 20. Effect of temperature on the stress-strain behavior of X-8 at 0.1 in./in./min.

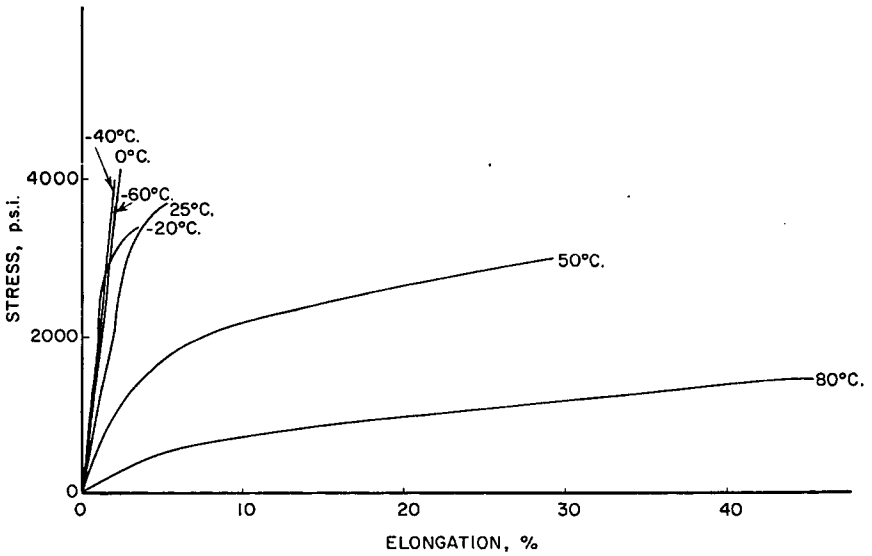

Fig. 21. Effect of temperature on the stress-strain behavior of OGK at high rate.

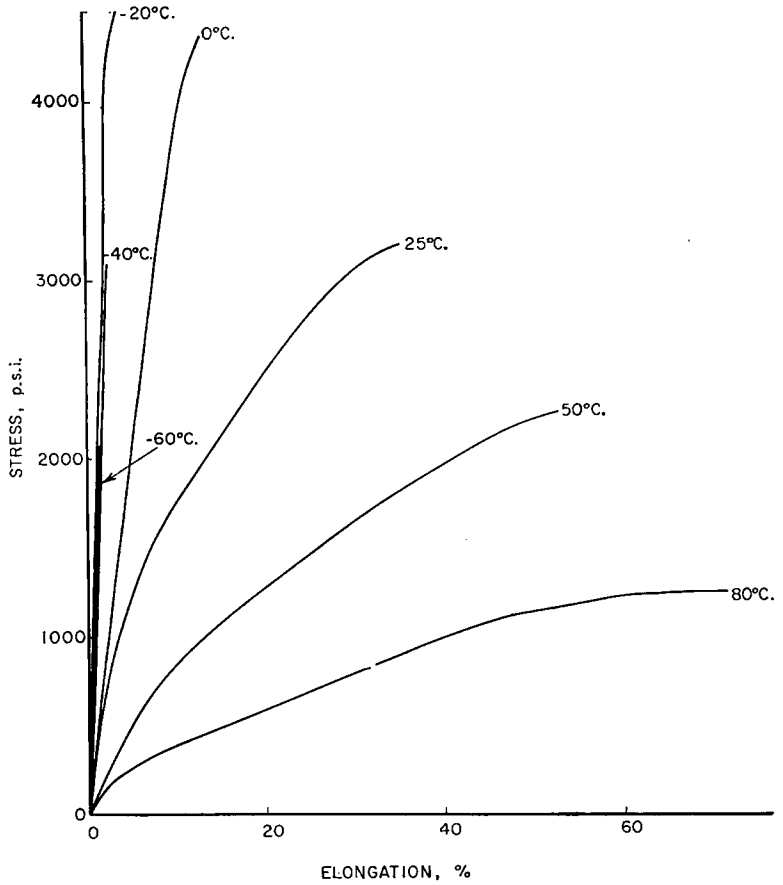

Fig. 22. Effect of temperature on the stress-strain behavior of ARP at high rate.

and consequently the temperature of the material is increased. This then tends to reverse the previous effect.

It is entirely possible that this effect exerts considerable influence on the ARP results. At the slower rates appreciable flow is noticed. Then, as the rate is increased, the latter portion of the curve becomes practically a straight line and each successive curve shows a rapidly increased slope to failure. However, at the highest rate, a change is noted and the slope of the stress-strain curve decreases sharply before failure.

From these results it may be concluded that both temperature and rate of loading greatly affect the response of propellant formulations to tensile loading. However, from the wide variations noted in the behavior of the formulations studied, it must be concluded that there is no simple way of predicting performance at one rate (or temperature) from performance at another rate (or temperature).

No continuous (i.e., predictable) relationships exist between rate of loading and such strength characterics as log time to failure, work to

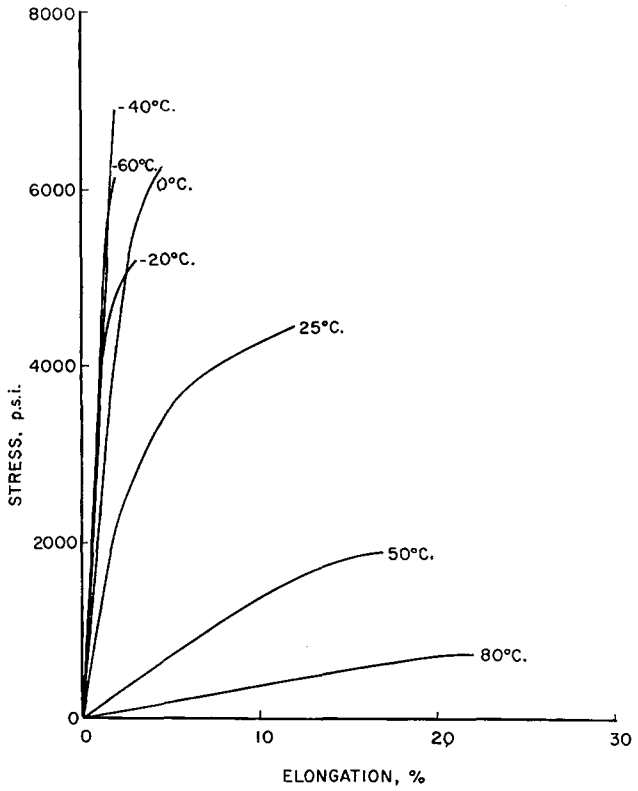

Fig. 23. Effect of temperature on the stress-strain behavior of T-16 at high rate.

produce failure, and modulus of elasticity. Marked discontinuities and reversals of trend are evident in all curves representing these relationships for the four propellants studied (OGK, ARP, X-8, and T-16). The general finding that strength tends to increase with rate of loading is not consistently supported by the results of this study. The curves for three of the four propellants tend to level off at the higher loading rates, and one formulation (OGK) even shows decreasing strength at the highest rate levels studied.

Similarly, the curves obtained for performance of the four propellants at various temperatures under both high rate and low rate (or "static") loading conditions show no consistent or continuous trends or relationships between strength and temperature at high or low rates of loading.

Appendix I

The overall view of the Plastics and Packaging Laboratory equipment utilized for tests in which times to failure are too short to be conducted on the conventional static testing equipment is shown in Figure 25. This figure shows a standard Type I ASTM D638 plastic specimen in position for

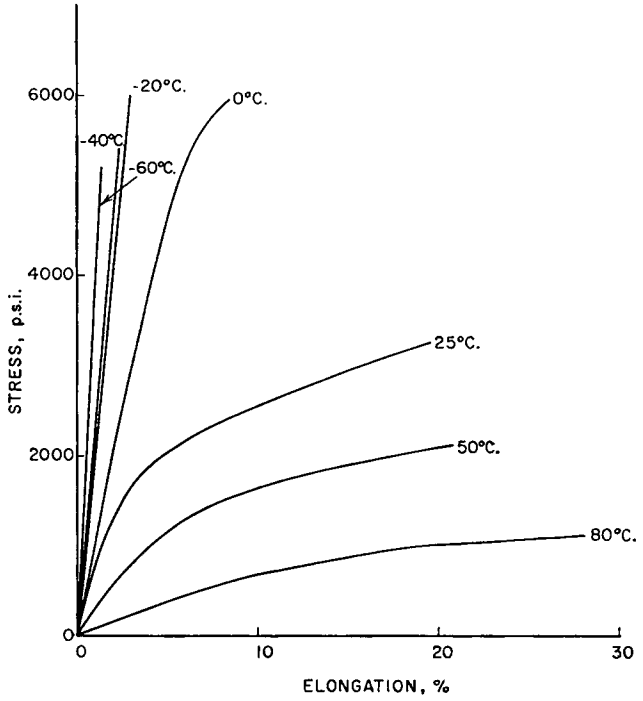

Fig. 24. Effect of temperature on the stress-strain behavior of X-8 at high rate.

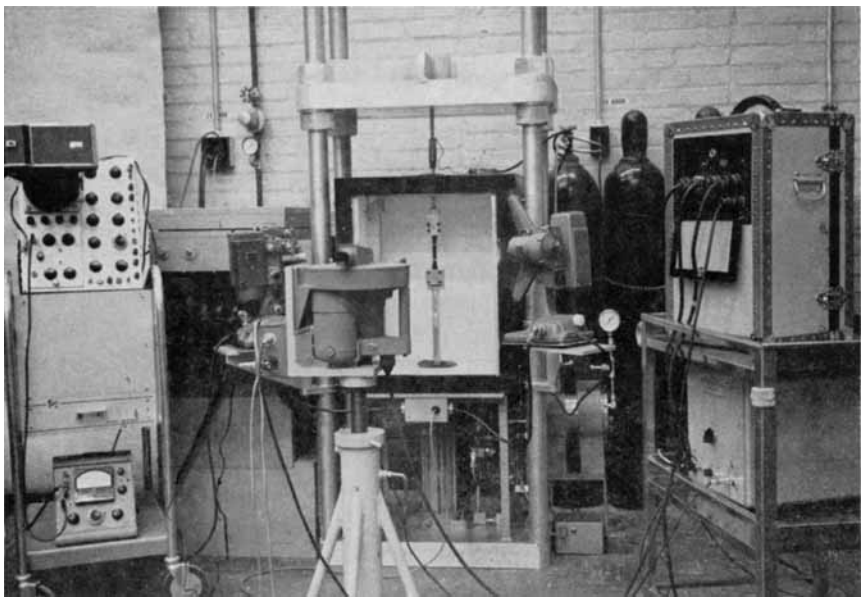

Fig. 25. Overall view of high rate testing equipment.

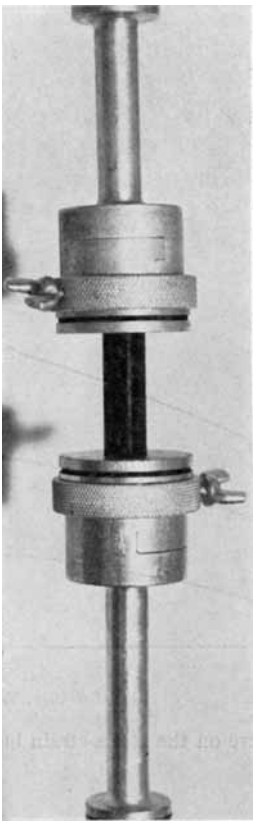

Fig. 26. Close up of specimen in machine ready for testing.

testing. High pressure gas is admitted from a reservoir to the upper side of a piston by means of a solenoid valve. This piston travels in a cylinder containing slots in the center portion. By the time that the upper side of the piston reaches the slots, the specimen is broken and the gas escapes as the slots are exposed. As the bottom of the piston passes beyond the bottom of the slots, the air in the bottom of the cylinder is compressed and acts as a cushion to stop the downward travel of the piston. A second line from the reservoir to the upper side of the piston, in addition to incorporating a solenoid valve, also contains a needle valve. This allows regulation of the gas flow to permit testing at slower rates. In this manner the range of failure times from those obtainable with the conventional static machines to the millisecond range may be covered.

The load measuring system consists of an SR-4 gaged cylindrical weighbar located above the upper grip. After suitable amplification, the signal from the instrumented weighbar is displayed on an oscilloscope, and the load versus time trace is photographed by a Polaroid camera.

The deformation is recorded by use of a high speed camera capable of operating up to 16,000 pictures/sec. By following the separation of gage

marks, in this case marks on the specimen grips, a continuous record of the test is obtained. Timing marks are placed on the edge of the film by a pulse generator so that a deformation vs time record is obtained. By crossplotting these two records, a stress-strain curve may be obtained.

For other than room temperature testing a door is placed on the front of the temperature control cabinet. This contains a polymethylmethacrylate pane in the center through which the high speed motion picture

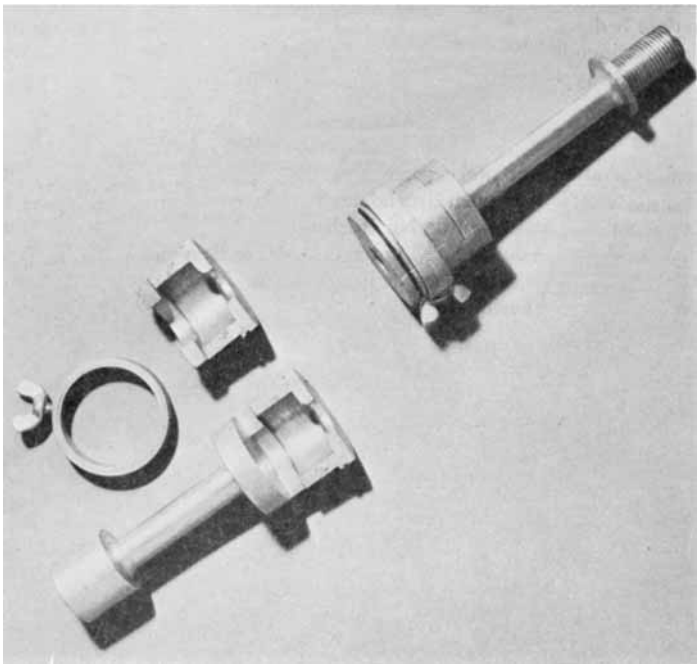

Fig. 27. Detail of grips used for propellant specimen.

camera may photograph the specimen deformation. Also located in the door are two polymethylmethacrylate rods which transmit light to the specimen area from two exterior sources thus providing the required illumination for photography.

Appendix II

The JANAF standard dumbbell specimen used for the propellant testing is a shoulder suspended type. The gage section is $^1/_2$ in. in diameter and 2 in. in length. The ends are each 1 in. in diameter and are connected to the gage section by a $^1/_8$ in. radius.

The specimen, ready for testing, is shown in Figure 26. Figure 27 shows one of the grips opened for insertion of the specimen. The line on the outside of the grips corresponds to the location of the shoulder of the specimen and is used as the reference for deformation measurement.

All specimen were machined from representative grains and were selected such that each group contained no two specimens taken from the same location within any one grain.

Résumé

On a étudié les propriétés de tension de combustibles propulseurs solides pour fusées, dont deux obtenus par coulés, deux autres par extrusion. Cette étude a été effectuée à 25°C et à 50% R.H. pendant des durées de chute variant de 0.005 à 2.500 sec. Les effets de la température ont également été étudiés à la vitesse la plus élevée et à 0.1 in/in/min dans le domaine de température −60 à 80°C. Les résultats montrent que la température ainsique la vitesse de charge affectent fortement les propriétés de tension des propulseurs du type double-base.

Zusammenfassung

Die Zugeigenschaften von zwei gegossenen und zwei extrudierten festen Raketentreibstoffen wurden bei 25°C über einen Bruchdauerbereich von 0,005 bis 2500 sek untersucht. Der Einfluss der Temperatur wurde bei Höchstgeschwindigkeit und bei 0,1 in/in/min über einen Bereich von −60 bis 80°C untersucht. Die Ergebnisse zeigen, dass sowohl Temperatur als auch Belastungsgeschwindigkeit die Zugeigenschaften von doppelbasigen Treibstoffen sehr beeinflussen.